RSC Advances

ROYAL SOCIETY OF CHEMISTRY

www.rsc.org/advances

Ultra sensitive and wide-range pH sensor based on the BSA-capped Cu nanoclusters fabricated by fast synthesis through the use of hydrogen peroxide additive

Liao Xiaoqing,[a] Li Ruiyi[a] and Li Zaijun*[a,b]

[a] *School of Chemical and Material Engineering, Jiangnan University, Wuxi, 214122, China*

[b] *The University of Birmingham, Edgbaston, Birmingham, BI5 2TT, United Kingdom.*

The study reported a new pH sensor based on the BSA-capped copper nanoclusters fabricated by fast synthesis through the use of hydrogen peroxide additive. The hydrogen peroxide destroys part peptide and disulfide bonds in BSA molecule and creates a better protonation/deprotonation system. The proposed pH sensor provides a better sensitivity and wider range of pH response compared with other metal nanoclusters reported in literatures.

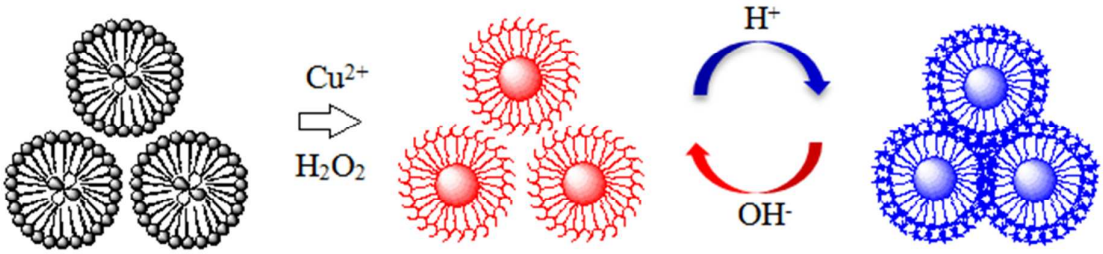

Cite this: DOI: 10.1039/c0xx00000x

www.rsc.org/xxxxxx

ARTICLE TYPE

Ultra sensitive and wide-range pH sensor based on the BSA-capped Cu nanoclusters fabricated by fast synthesis through the use of hydrogen peroxide additive

Liao Xiaoqing,[a] Li Ruiyi[a], Long Xiaohuan[a] and Li Zaijun*[a,b]

Received (in XXX, XXX) Xth XXXXXXXXX 20XX, Accepted Xth XXXXXXXXX 20XX
DOI: 10.1039/b000000x

The accurate estimation of pH in environment and on cellular level is important in environmental, biomedical and bioprocess applications. Herein, we reported an ultra sensitive and wide-range pH sensor based on the BSA-capped Cu nanoclusters (CuNCs) fabricated by fast synthesis through the use of hydrogen peroxide additive. Owing to strong oxidation capacity, hydrogen peroxide destroy part peptide and disulfide bonds in the BSA molecule and results in an increased exposure of hydrophilic groups capable of protonation, which will greatly accelerate the formation of CuNCs and improve the response of CuNCs towards pH fluctuation in the surrounding environment. The results demonstrate that the repulsion development and conformational change of BSA with decreasing pH value induce the aggregation of CuNCs, leading to color change and fluorescence quenching of the CuNCs at low pH value. The fluorescence intensity exhibits a linear fashion over the pH range of 2-14 and increases by around 20-fold approximately with a greater fluorescence at a higher pH value. The sensitivity and pH range are much better than other metal nanocluster pH sensors reported in literatures. The pH probe is also sensitive to different buffer solution except for those containing some ions that could react with CuNCs. The ionic strength of buffers has a little influence on the pH-responsive behaviour. The proposed pH sensor has been successfully applied for measuring pH value on natural water and on intracellular RBL-2H3 cells. The study also provides a promising candidate in the applications in biological, medical and pharmaceutical fields.

1 Introduction

Even though very small variations in pH value can devastate lives of plants and animals. In our surroundings, acid rain, excessive human activities and untreated sewage may cause environmental pH value changes and the acidification of soils, streams, lakes and seawater, which will further pollute our drinking water.[1] In life science, intracellular pH is an essential parameter for cell, enzyme and tissue activities, which plays a vital role in cell metabolism processes, including proliferation and apoptosis.[2] As abnormal intracellular pH value is related to improper cell function and growth, they may affect human physiology such as cancers and neurological disorders, measuring pH distribution and fluctuation with high temporal-spatial resolution in the living cells is essential for advancing our understanding of cell biology.[3] Thus, the accurate estimation of pH in environment and on cellular level is important in environmental, biomedical and bioprocess applications.[4]

The unique property of metal nanoclusters attracts great attention due to their molecule-like behaviour, including discrete electronic states and size-dependent fluorescence. The intensity and wavelength of fluorescence are highly sensitive to surrounding environments, which have made nanoclusters as attractive functional materials in the development of versatile sensors.[5] To date, studies have been made in pH-responsive optical properties of metal nanoclusters such as silver nanoclusters,[6] gold nanoclusters,[7] copper nanoclusters,[8] silicon nanoclusters,[9] cerium/gold nanoclusters[10] and gold/copper nanoclusters.[11] The proteins at high concentrations were often applied as the template and reducing agent for building on stable and biocompatible metal nanoclusters. Bovine serum albumin (BSA) is most popular. There are 28 cysteine and 20 tyrosine residues for each BSA molecule, leading to a greater capping and reducing capabilities. Many investigations have demonstrated that the pH response of metal nanoclusters strongly depends on features of the template, including its charge density and protonation level.[12] However, BSA-capped nanoclusters often possess pH-insensitive fluorescence property because of its low exposed degree of hydrophilic groups capable of protonation.[13] The study reported a new fluorescent pH sensor based on the BSA-capped copper nanoclusters (CuNCs) fabricated by fast synthesis through the use of hydrogen peroxide additive. The addition of hydrogen peroxide destroys part peptide and disulfide bonds in BSA molecule, which increases the exposure of hydrophilic groups capable of protonation. The action greatly accelerates the formation of CuNCs and improves the response of the CuNCs towards pH fluctuation in the surrounding

environment. The as-prepared pH sensor provides an advantage of high sensitivity, wide pH range and excellent reversibility compared with other metal nanoclusters.

2 Experimental

2.1 Materials

Bovine serum albumin (BSA), hydrogen peroxide (H_2O_2), copper sulphate ($CuSO_4$) and sodium hydroxide (NaOH) were purchased from Sigma-Aldrich (Mainland, China). Britton-Robinson buffer solution (BR buffer, H_3PO_4-HAc-H_3BO_3, 0.04 M) was prepared and its pH value was adjusted using 0.2 M NaOH solution. Phosphate-buffered saline (PBS, pH7.0, Na_2HPO_4-KH_2PO_4-NaCl-KCl, 0.01 M) was prepared in the laboratory. Other reagents were of analytical regent grade and purchased from Shanghai Chemical Company (Shanghai, China). Ultrapure water (18.2 Ω cm) purified from Milli-Q purification system was used throughout the experiment.

2.2 Apparatus

Transmission electron microscope (TEM) image was conducted on a JEOL 2010 FEG microscope at 200 keV. The sample was prepared by dispensing a small amount of dry powder in ultrapure water. Then, one drop of the suspension was dropped on 300 mesh copper TEM grids covered with thin amorphous carbon films. The pH was measured on the PHS-3D pH meter (Shanghai Precision Scientific Instruments Co., Ltd., China). Fluorescence spectrum and intensity were recorded on a Cary Esclipse fluorescence spectrophotometer (Agilent, Japan). Circular dichroism (CD) measurements were performed on a MOS-450 circular dichroism spectrometer using a 0.01 cm quartz cell. The percentage of various conformations has been determined for both CuNCs and CuNCs-c by using SELCON3 analysis programme. The zeta potential measurements were carried out in a ZETASIZER2000 Zeta Potential Analyzer.

2.3 Synthesis of CuNCs

The $CuSO_4$ solution (10 ml, 20 mM) was added into the BSA solution (50 ml,15 mg ml^{-1}). After stirred for 5 min, its acidity was slowly adjusted to pH 12 using the NaOH solution (1 M). Then, the H_2O_2 solution (10 ml, 0.4 M) was injected into the above solution under a vigorous agitation. After that, the mixed solution was heated at 55°C for 1 h to obtain the CuNCs solution. For the comparison, a control sample (termed as CuNCs-c) was also prepared by using the same procedure unless no addition of H_2O_2.

2.4 Procedure for measuring pH value

The CuNCs solution (200 µl) was mixed with the BR buffer (600 µl). After a 5 min incubation, it was subjected to fluorescence measurements on the fluorescence spectrophotometer with the excitation wavelength of 320 nm and the emission wavelength of 420 nm. The fluorescence signal was monitored by using a photomultiplier tube on the fluorescence spectrophotometer and was recorded by computer. For the each of pH detection, the fluorescence measurement was repeated thrice, and the average fluorescence signal was obtained in the study.

2.5 Method for studying on the interference of ionic strength

The CuNCs solution (200 µl) and different concentration of NaCl solution (200 µl) was mixed with the BR buffer (pH 10.1, 400 µl). After 5 min, the fluorescence was measured and recorded on the fluorescence spectrophotometer with the excitation wavelength of 320 nm and the emission wavelength 420 nm.

2.6 Zeta potentials measurement

The zeta (ζ) potentials of CuNCs was examined by dynamic light scattering (DLS) as a function of pH value. The DLS sample was prepared as follows: the CuNCs solution (100 µl) was diluted in the BR buffer (pH 2-14, 2.9 ml). Then, the mixed solutions was passed through millipore filters with a pore size of 0.22 µm to remove dust. The zeta potential of the solution was carried out on the Zeta Potential Analyzer.

2.7 The pH-dependent intracellular fluorescence imaging

RBL-2H3 cells in Roswell Park Memorial Institute 1640 (RPMI 1640) medium supplemented with 10% fetal BSA were added to each well of a 48-well plate (200 µl per well). The cells were cultured first for 24 h in an incubator (37°C, 5% CO_2), and for another 24 h after the culture medium was replaced with 300 µl of RPMI 1640 containing 30 µl of the CuNCs. Before imaging, the CuNC-loaded cells were rinsed three times and incubated with 1.0 ml of BR buffer at various pH values for 10 min. Cells were imaged with a DSU live-cell confocal microscope (Olympus, Japan) system with laser excitations of DAPI, and the images were analyzed using image-Pro Plus software.

3 Results and discussion

3.1 Fluorescent characteristics

A new strategy has been successfully developed for fast synthesis of the CuNCs through the use of H_2O_2 additive. The result verifies that the addition of H_2O_2 greatly accelerates the formation of CuNCs. The synthesis of CuNCs is reduced to less than 1 hour. The time is much less than the conventional method in the absence of H_2O_2 (about 30 days). In the study, we focus on fluorescent characteristics of the resulting CuNCs. Fig.1 presents typically fluorescence spectra of the CuNCs and the CuNCs-c. Two kinds of CuNCs products give very similar fluorescence spectrum with the same shape and maximum emission wavelength, verifying that two kinds of CuNCs have analogical nanostructure and similar particle size distribution. Interestingly, the CuNCs offer a higher fluorescence intensity than the CuNCs-c. Our study

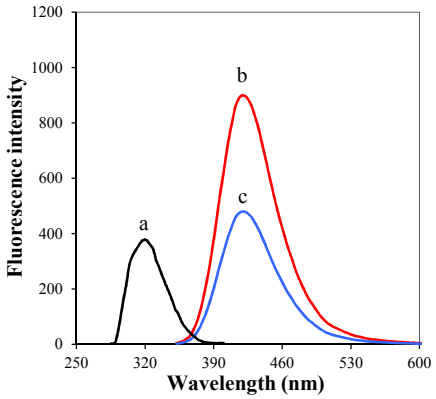

Fig.1 Excitation spectrum (a) of the CuNCs and fluorescence spectra of the CuNCs (b) and the CuNCs-c (c)

reveals that the CuNCs-c exists a high concentration of Cu^{2+} due to weak reducing ability of BSA. The residual of Cu^{2+} will not only bring a low content of CuNCs but also quench part fluorescence, resulting that the CuNCs-c exhibit a relatively low fluorescence intensity. The result demonstrates that the addition of H_2O_2 during the synthesis of CuNCs brings an enhanced fluorescence intensity.

Solvation dynamics of the as-prepared CuNCs was studied by measuring the fluorescence spectra with different excitation wavelength. Fig.2 indicates that the fluorescence emission peak changes with the change of excitation wavelength. When the excitation wavelength was changed from 320 to 420 nm, its emission spectrum was wavelength-tunable with the emission maximum shifting from 410 nm to 480 nm (shown in Fig.s1). The fluorescence intensity decreases with the increase of excitation wavelength. Such a strong excitation wavelength dependent fluorescence in the CuNCs is originated from "giant red-edge effect".[14] When the CuNCs are present in a polar solvent, the solvation dynamics slows down to the same time scale as the fluorescence due to local environment of the CuNCs. Giant red-edge effect of the CuNCs disappears in a nonpolar solvent, thus leading to a narrow fluorescence peak that is independent of the excitation wavelength. The discovery of underlying strong excitation wavelength dependent fluorescence mechanism offers guidelines for development of the CuNCs-based optical devices. The result also demonstrates that fluorescence of the as-prepared CuNCs is sensitive to environment polarity.

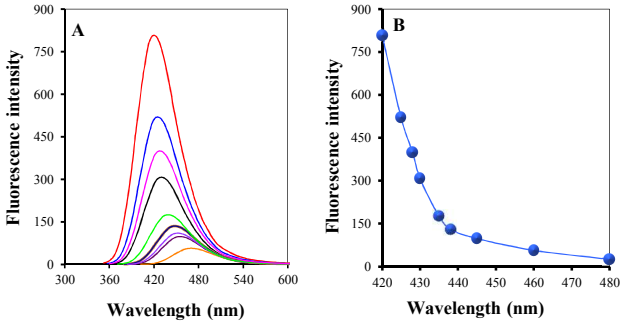

Fig.2 Fluorescence spectra (A) of the CuNCs with the excitation wavelength of 320, 335, 340, 345,355, 360, 380, 400 and 420 nm (from top to bottom) and relationship curve (B) of the emission wavelength with the fluorescence intensity

3.2 Response towards pH value

Sensing performance of the as-prepared CuNCs is characterized by fluorescence measuring in the BR buffers from pH 2 to 14. Fig.3 shows that the CuNCs are highly sensitive to the pH value adjusted by the BR buffer. The fluorescence intensity will rapidly increase with the increase of the pH value in the surrounding environment. The fluorescence signal reaches the maximum value at pH 14, which is more than 20-fold that at pH 2. Further, Fig.3B indicates that the fluorescence intensity changes in a linear fashion over the pH range from 2 to 14. The linear equation is following equation: F=92.56pH-221.25 and the corresponding correlation coefficient is about 0.9971. For the comparison, the analytical characteristics of other metal nanoclusters pH sensors reported in literatures were listed in Table 1. From Table 1, we can observe that the CuNCs as novel pH sensor provides the best sensitivity and the widest range of pH response. Thus, the as-prepared CuNCs can be widely applied for measuring the pH value in environmental and life samples. Moreover, Fig.3B also shows that the sensitivity and pH range of the CuNCs are much better than that of the CuNCs-c. This is because a low fluorescence intensity of the CuNCs-c leads to a relatively low sensitivity towards the pH response compared with the CuNCs. besides, a relatively high isoelectric point and low

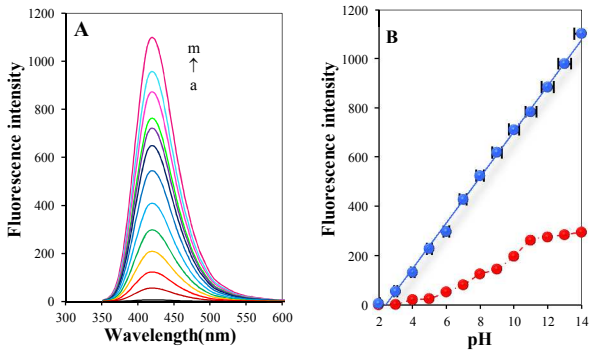

Fig.3 Fluorescence spectra (A) of the CuNCs at pH 2, 3, 4, 5, 6, 7, 8, 9.10, 11, 12, 13 and 14 and the relationship curves (B) of fluorescence intensity of CuNCs (upper) and CuNCs-c (under) at 420 nm with the pH values.

exposure of hydrophilic groups capable of protonation result in a narrow pH-sensitive range of the CuNCs-c. The results also confirm that the introduction of H_2O_2 in the synthesis obviously improves the pH dependent optical properties.

Table 1 Analytical characteristics of metal nanocluster pH sensors

Nanocluster	Stabilizer	Sample	pH range	Sensitivity	Ref.
Ce/AuNC	BSA	He La cells	6-9	2	10
AgNC	poly-ethylenimine		5.02–7.96	10	12
AuNC	glutathione and citrate	cells	4.1-8.6		7
CuNC	BSA+hydrazine hydrate	CAL-27 cells	6-12		15

The as-prepared CuNCs also display a distinct color variation with the pH dropping (shown in Fig.4), such as from red (basic medium) to orange color (neutral medium) and finally to yellow color (acid medium). At the same time, its fluorescence intensity reduces with the decrease of pH value. This imparts an excellent characteristic to this probe as a color indicator in the pH detection. From Fig.4, we observe that the CuNCs solution is transparent and no any precipitation can be found when the pH value is more than 4.01, indicating an excellent water-solubility. When the pH value reduce to 4.01, BSA begin to precipitate from the CuNCs solution. The precipitation reaches its maximum at pH 2.36, indicating an isoelectric point of about 2.36 for the BSA in the CuNCs system. The isoelectric point is lower than that of BSA in the CuNCs-c system (about 3.26) (shown in Fig.s2). The result demonstrates that the introduction of H_2O_2 during the synthesis decrease the isoelectric point of BSA. This is mainly because the use of H_2O_2 destroys part peptide and disulfide bonds due to its strong oxidation capacity, which enhances the water-solubility and leads to the decrease of the isoelectric point. Interestingly,

Fig.4 Photographs for recording color changes of the CuNCs in BR buffer at different pH value under visible light (upper) and UV light (under).

the precipitation formed in the acid medium can be dissolved in the base medium and the solution color became red and transparent again.

To test respond of the as-prepared CuNCs to pH change, the amounts of the CuNCs solution was well mixed with the BR buffer (pH 7 or 10) and then its fluorescence signal was immediately measured on the fluorophotometer. The result shows that the fluorescence intensity reaches the maximum value within 20 s, indicating a very fast respond to pH change. Further, the effect of the standing time on the fluorescence intensity was investigated in the laboratory. Fig.s3 indicates that the fluorescence intensity can keep almost unchanged within 60 min at least, indicating an excellent stability for pH measurement.

To further investigate reversibility of the CuNCs, the pH value was changed from 11.13 to 3.01 and again to 11.13 using acid and base as the modulators. The fluorescence intensity was measured at the each pH value and results were shown in Fig.5. It can be seen that the cycles can be repeated 7 times without obvious fatigue. A little decrease of fluorescence intensity was observed for the reason that the volume of solution became larger after each cycle. The reversibility of the CuNCs in strong acid (1 M HCl) and strong base (5 M NaOH) medium was tested in the study. The result shows that the fluorescence in strong acid and strong base medium can rapidly be restored by adjusting the pH value using strong acid or strong base solution, indicating an excellent reversibility. Based on the excellent reversibility, we think that the aggregation at a low pH value don't influence on the crystal structure and particle size of the cores in the CuNCs. The formed soft agglomeration is easy to dissociate into the pristine CuNCs. Thus, the fluorescence intensity can rapidly increase in a high pH value. All of these afforded significant evidences and advantages to the CuNCs for the applications in various environments.

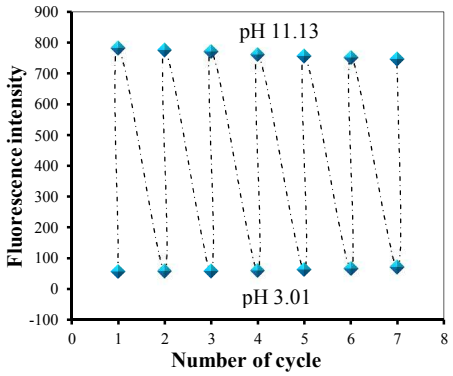

Fig.5 Fluorescence intensity of the CuNCs reversibly went upward and downward by alternating the pH value. One cycle meant that the fluorescent intensity was measured as the value changed from pH 11.13 to 3.01 and then from pH 3.01 to 11.13

The proposed pH sensor was also sensitive to other commonly used buffer solutions such as tris(hydroxymethyl)aminomethane-HCl buffers (Tris-HCl), acetic acid-sodium acetate buffer (HAc-NaAc), phosphate buffer (PB buffer) and borax-HCl buffer (shown in Fig.s4). Good corresponding linear relationships were obtained between the pH values measured by pH meter and fluorescence intensity of the CuNCs, revealing that the fluorescence intensity changes were primarily due to the variation of the pH values rather than the reaction between the CuNCs and the ions contained in the buffer solutions. More importantly, the CuNCs would react with some anions contained in the buffer solutions, resulting in deviations in the pH determination. In spite of this, the pH-responsive action would not be affected by the ionic strength. The fluorescence intensity of CuNCs remained almost constant when exposed to 0.0-1.0 M NaCl solutions (shown in Fig.6), indicating the ionic strength had no significant effect on the pH sensor.

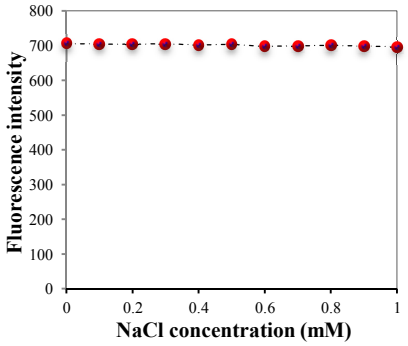

Fig.6 Fluorescence peak intensity of the CuNCs at the BR buffer solution of pH10.1 containing different concentration of NaCl

3.3 Mechanism for pH Response

Resonance light scattering (RLS), Zeta potential, transmission electron microscope (TEM) and circular dichroism (CD) of the as-prepared CuNCs in different pH values were investigated to understand the response mechanism towards pH value. Fig.7**A** displays RLS spectra of the CuNCs at different pH value. It can be seen that RLS spectra of the CuNCs in different pH values gives a similar shape. However, the RLS intensity highly depends on the pH value. When the pH value is close to the isoelectric point of BSA, the PLS intensity rapidly increases with the decrease of pH value. This is because the loss of charge results in an obvious aggregation process, indicating a strong RLS signal. The BSA on the CuNCs surface is negatively charged in the base aqueous solution with the increase of pH value, which is stabilized against aggregation due to the negative electrostatic repulsion. Thus, the BSA on the CuNCs surface indicates a relatively weak RLS intensity at pH 8 and 12.

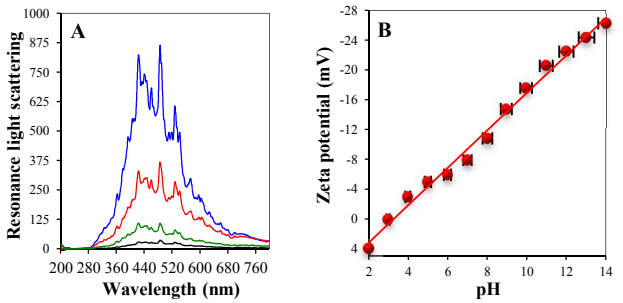

Fig.7A: Resonance light scattering spectra of the CuNCs at pH 3, 5, 8 and 12 (from top to bottom). Condition: λex=λem (290-800nm). B: The relationship curve of zeta potentials of CuNCs with the pH value.

Fig.7**B** presents the relationship curve of the Zeta potential of the CuNCs with pH values. Zeta potential of the as-prepared CuNCs is sensitive to the pH values in the solution. The CuNCs exhibits a positive Zeta potential when the pH value is less than 2.36, indicating a positive charge attached on the surface of CuNCs. The Zeta potential is equal to zero at pH 2.36, indicating an isoelectric point of 2.36. The isoelectric point is lower than that of BSA (4.01). This is attributed the use of H_2O_2 during the synthesis of CuNCs destroys part chemical bonds in BSA and results in an enhanced exposure of hydrophilic groups capable of protonation. When the pH value is more than 2.36, the Zeta potential of CuNCs becomes negative charge, indicating a negative charge attached on the CuNCs surface. The negative charge is beneficial to improve the stability of the CuNCs solution due to their electrostatic repulsion. Interestingly, the Zeta potential (ζ) linearly increases with the increase of the pH value in the solution in the range from 2 to 14. The linear equation is following equation: ζ(mV)=-2.513pH+8.23 and the corresponding correlation coefficient is 0.9918. Thus, the pH value can be detected by measuring the Zeta potential.

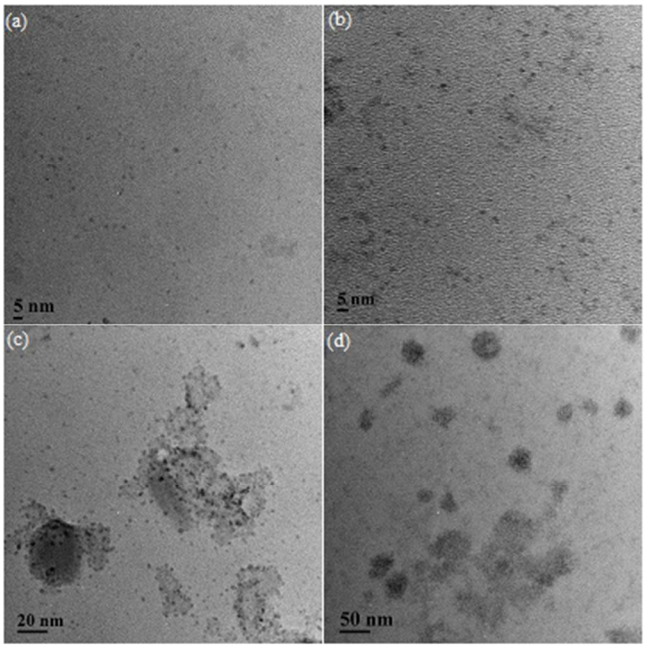

Fig.8 TEM images of the CuNCs at pH 12 (a), 8 (b), 5 (c) and 3 (d)

Fig.8 presents typically TEM images of the as-prepared CuNCs at different pH value conditions. From Fig.8, we can observe that the CuNCs have a narrow particle size distribution with an average diameter of 1.6±0.5 nm at the pH 12. However, the particle size of CuNCs will increase with reduce of the pH value. When the pH value is close to 5, an obvious aggregation appears in the CuNCs. Interestingly, the aggregation will rapidly disappear if the pH value was adjusted to base level, verifying that the aggregation is a reversible process.

Fig.9 presents the ratio of secondary structure in the BSA in the CuNCs and CuNCs-c. BSA in the CuNCs exhibits an obvious reduce of α-helix and increase of unordered. This should be attributed to the use of H_2O_2 during the synthesis of CuNCs. Many investigations have confirmed that H_2O_2 can be changed into •OH radical in the catalysis of metal ions such as Cu^{2+}.[16] Due to better oxidation ability compared with H_2O_2, •OH could partly destroy the peptide and disulfide bonds in BSA and results in a bigger exposure of hydrophilic groups capable of protonation.[17] Accompanied by the formation of CuNCs, hydrophobic groups in BSA are embedded in the structure center and its hydrophilic groups are distributed in the surface of CuNCs, which will improve the response of the CuNCs towards pH fluctuation in the surrounding environment.

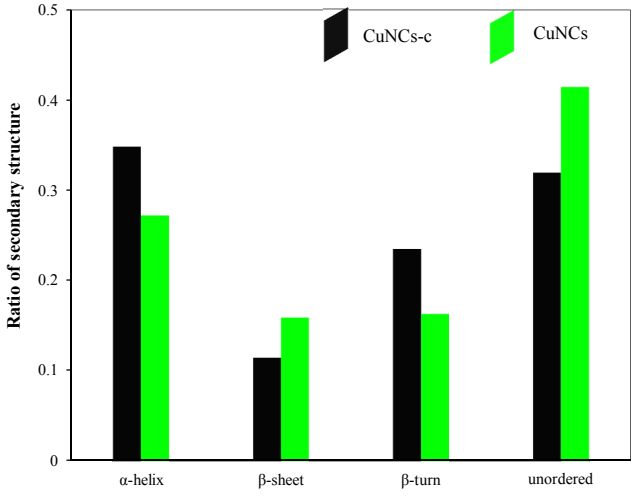

Fig.9 The secondary structure of CuNCs and CuNCs-c

Basing on the above analysis, we suggest a mechanism for pH response. The pH response of CuNCs is originated from their reversible aggregation. At a low pH value, the aggregation get further development. This helps to transfer energy between CuNCs due to their very small distance and results in the decrease of the fluorescence intensity. In addition, the protonation of BSA on the CuNCs surface at low pH value leads to partly quench the fluorescence due to its electron withdrawing effect. At a high pH value, the aggregation is greatly suppressed by their electrostatic repulsion. More negatively charged ions such as OH^- were adsorbed on the surface of CuNCs. Their electron donating effect enhances the fluorescence intensity. More importantly, the use of H_2O_2 during the synthesis breaks up part peptide and disulfide bonds in BSA and results in increasing exposure of hydrophobic groups capable of protonation. The action creates an elaborate protonation/deprotonation system in the CuNCs, which further improves the range and sensitivity of the response of pH sensor towards the pH value.

3.4. Detection of pH value in water samples

The pH-sensitive properties of the fluorescence emission of the CuNCs could be applied in the pH detection of bodies of water to check if the water is polluted or if it is safe to drink. Comparing the results from our method and pH meter, as shown in Table 2, we can see that the result is reliable and the CuNCs can be utilized as an excellent fluorescent pH indicator for real water samples.

Table 2 The results for the detection of pH value in water samples (N=5)

Sample	The results obtained by proposed method	The results obtained by pH meter
River water	7.33±0.12	7.29 ±0.18
Lake water	6.90 ±0.09	6.84 ±0.13
Tap water	6.82 ±0.15	6.90 ±0.22
Well water	7.13 ±0.05	7.09 ±0.14
Rain water	6.81 ±0.08	6.92 ±0.05
Distilled water	7.04 ±0.10	7.06 ±0.16

3.5 Intracellular pH sensing by confocal microscopy

To further demonstrate the application of the probe in live cells, the intracellular calibration experiment was made in CuNCs-loaded RBL-2H3 cells. In the process of intracellular pH sensing, CuNCs have two roles: the signal molecule for pH sensing and the carrier for carrying itself as a single molecule to enter the cells. This could prevent any complicated modification processes. Fig.10 shows the confocal images of RBL-2H3 cells treated with the BR buffer, the CuNCs are well-distributed in live cells, indicating excellent membrane permeability due to their small size. The CuNCs-loaded cells exhibit a weak fluorescence in pH 5.7 BR buffer for the DAPI channel, nevertheless, the RBL-2H3 cells become brighter as the pH increases. The fluorescence intensity increases with pH from 5.1, 6.6, 7.2 to 8.0. All of these results establish that the obtained CuNCs are desirable pH probes for monitoring the pH changes in live cells.

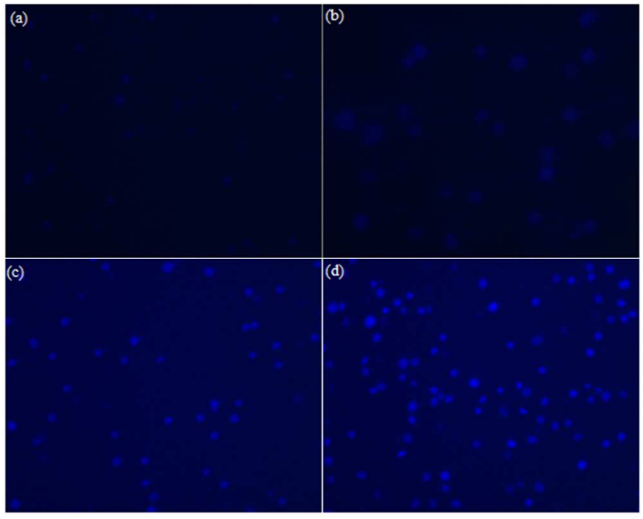

Fig.10 Epifluorescence microscopic image of RBL-2H3 cells treatment with the CuNCs (20 μg ml^{-1}) at pH 5.1(a), 6.6 (b), 7.2 (c) and 8.0 (d) using the UV excitation of 365 nm.

4. Conclusions

We have successfully developed an ultra sensitive and wide-range pH sensor based on the BSA-capped copper nanoclusters fabricated by fast synthesis through the use of hydrogen peroxide additive. Owing to strong oxidizing capacity of hydrogen peroxide in the presence of Cu^{2+}, part peptide and disulfide bonds in the BSA molecule were broken up during the synthesis. This leads to increase exposure of hydrophilic groups capable of protonation in the BSA molecule, helping to create a better protonation/deprotonation system for the copper nanoclusters compared with the synthesis in the absence of hydrogen peroxide. The proposed pH sensor exhibits an enhanced response towards pH fluctuation in the surrounding environment. The applications of the CuNCs for the pH detection in natural water and imaging in live RBL-2H3 cells were successfully achieved, proving that they can reveal intracellular pH fluctuations via a change in the fluorescence intensity response. The study also provides a promising candidate in the applications in biological, medical and pharmaceutical fields

Acknowledgments

The authors acknowledge the financial support from the National Natural Science Foundation of China (No.21176101), the Fundamental Research Funds for the Central Universities (No. JUSRP51314B)，MOE & SAFEA for the 111 Project (B13025) and the country “12th Five-Year Plan” to support science and technology project (No. 2012BAK08B01).

Notes and references

[a] *School of Chemical and Material Engineering, Jiangnan University, Wuxi, 214122, China. E-mail: zaijunli@263.net.*
[b] *The University of Birmingham, Edgbaston, Birmingham, BI5 2TT, United Kingdom.*

1 Z. Y. Yang, W. Qin, J. W. Y. Lam, S. Chen, H. H. Y. Sung, I. D. Williams and B. Z. Tang, *Chem. Sci.*, 2013, **4**, 3725.
2 M. Weinlich, U. Heydasch, F. Mooren and M. Starlinger, *Res. Exp. Med.*, 1998, **198**, 73.
3 A. M. Dennis, W. J. Rhee, D. Sotto, S. N. Dublin and G. Bao, *ACS Nano*, 2012, **6**, 2917.
4 H. R. Kermis, Y. Kostov, P. Harms and G. Rao, *Biotechnol. Prog.*, 2002, **18**, 1047.
5 X.F. Wu, R.Y. Li, Z.J. Li, J.K. Liu, G.L. Wang and Z.G. Gu, *RSC Adv.*, 2014, **4**, 24978; X.F. Wu, R.Y. Li and Z.J. Li, *RSC Adv.*, 2014, **4**, 9935.
6 Y.P. Zhong, C. Deng, Y. He, Y.L. Ge and G.W. Song, *Analytical Methods*, 2015, **7**, 1558; J.X. Dong, F. Qu, N.B. Li and H.Q. Luo, *RSC Adv.*, 2015, **5**, 6043.
7 R.J. Stover, A.K. Murthy, G.D. Nie, S. Gourisankar, B.J. Dear, T.M. Truskett, K.V. Sokolov and K.P. Johnston, Journal of Physical Chemistry C, 2014, **118**,14291; W.C. Ding, Y. Liu, Y.J. Li, Q.R. Shi, H.S. Li, H.B. Xia, D.Y. Wang and X.T. Tao, *RSC Adv.*, 2014, **4**, 22651.
8 W. Wang, F. Leng, L. Zhan, Y. Chang, X.X. Yang, J. Lan and C.Z. Huang, *Analyst*, 2014, **139**, 2990.
9 Y.L. Feng, Y.F. Liu, C. Su, X.H. Ji and Z.K. He, *Sensor Actuat. B-Chem.*, 2014, **203**, 795.
10 Y.N. Chen, P.C. Chen, C.W. Wang, Y.S. Lin, C.M. Ou, L.C. Ho and H.T. Chang, Chem. Commun., 2014, 50, 8571.
11 P.C. Chen, J.Y. Ma, G.L. Lin, C.C. Shih, T.Y. Lin and H.T. Chang, *Nanoscale*, 2014, **6**, 3503.
12 F. Gu, N.B. Li and H.Q. Luo, *Langmuir*, 2013, **29**, 1199.
13 P.-C. Chen, C.-K. Chiang and H.-T. Chang, *J. Nanopart. Res.*, 2013, **15**, 1336.
14 S.K. Cushing, M. Li, F.Q. Huang and N.Q. Wu, *ACS Nano*, 2014, **8** ,1002.
15 C. Wang, C.X. Wang, L. Xu, H. Cheng, Q. Lin and C. Zhang, *Nanoscale*, 2014, **6**, 1775.

16 T. Sun, H.R. Guo, H.L. Xu and B.K. Zhou**,** *Chemical Journal of Chinese Universities-Chinese*, 2007, 28, 856-858
17 M.M. Zou, Y. Li, J. Wang, J.Q. Gao, Q. Wang, B.X. Wang, P. Fan, *Spectrochimica Acta Part A: Molecular and Biomolecular Spectroscopy*, 2013, **112**, 206-213.